

---

# TINYTURBO: EFFICIENT TURBO DECODERS ON EDGE

---

S. Ashwin Hebbar<sup>1†</sup>

Rajesh Mishra<sup>2†</sup>  
Hyeji Kim<sup>2</sup>

Sravan Kumar Ankireddy<sup>2</sup>  
Pramod Viswanath<sup>1</sup>

Ashok Vardhan Makkuva<sup>1</sup>

## ABSTRACT

In this paper, we introduce a neural-augmented decoder for Turbo codes called TINYTURBO. TINYTURBO has complexity comparable to the classical max-log-MAP algorithm but has much better reliability than the max-log-MAP baseline and performs close to the MAP algorithm. We show that TINYTURBO exhibits strong robustness on a variety of practical channels of interest, such as EPA and EVA channels, which are included in the LTE standards. We also show that TINYTURBO strongly generalizes across different rate, blocklengths, and trellises. We verify the reliability and efficiency of TINYTURBO via over-the-air experiments.

## 1 Introduction

Codes form the backbone of the modern information age (WiFi, cellular, cable, and satellite modems). Some of the landmark codes include Reed-Muller (RM), BCH, Turbo, LDPC and Polar codes. In particular, Turbo codes have been widely used in modern communication systems and are part of 3G and 4G standards. While Turbo codes operate at near-optimal performance on the canonical additive white Gaussian noise (AWGN) channel, it is well known that the classical Turbo decoder [1] lacks robustness and performs poorly on non-AWGN channels. Thus designing turbo decoders with high reliability and robustness is of great interest.

In recent years, we have had tremendous achievements of deep learning (DL) across various disciplines such as computer vision and natural language processing. In particular, we have also seen impressive results from DL based decoders in channel decoding [2–10]. While these results demonstrate the potential of DL in designing optimal decoders, a majority of them still suffer from the huge computational complexity, which makes them intractable to be deployed in real-world communication systems.

Given this, more scalable approaches such as model-based DL has gained traction recently [11, 12]. One of the key ideas in this approach is to augment learnable parameters to existing channel decoders and train these parameters. A strong benefit of such neural decoders is that the complexity of the decoder does not increase much while reliability can be improved. In the context of Turbo codes, in a recent work [13], He et al. introduce TURBONET+, which augments learnable parameters to decoding every bit, and show that it improves the reliability of the classical Turbo decoders.

Despite the success of TurboNet+, there are three important open questions: (a) do we need all those learnable parameters, the number of which scales linearly in blocklength? (b) can we learn weights that generalize across rates, blocklengths, and codes and that are robust across channel variations? (c) what is the role of the learned weights? In this paper, we focus on addressing these questions. Our contributions are as follows.

- We propose TINYTURBO\*, a neural augmented Turbo decoder that has 18 trainable weights. We show that TINYTURBO recovers the reliability of the state-of-the-art neural augmented Turbo decoder, namely, TurboNet+ [13] which has 720 weights, for AWGN channels.

---

<sup>1</sup>University of Illinois, Urbana-Champaign

<sup>2</sup>University of Texas, Austin

<sup>†</sup>Equal contribution

Correspondance to: Ashwin, Rajesh <shebbar3@illinois.edu, rajeshkmishra@utexas.edu>

\* Code can be found at <https://github.com/hebbbarashwin/tinyturbo>

- We show the *robustness* of TINYTURBO: TINYTURBO outperforms TurboNet+ and the classical Turbo decoder for several practical channels.
- We demonstrate the strong *generalization* of TINYTURBO: TINYTURBO trained for rate-1/3 LTE Turbo codes of blocklength 40 performs well for Turbo codes with different blocklengths, rates, and trellises (e.g., blocklength 200, rate-1/2, Turbo-757).
- Our over-the-air experiment demonstrates that TINYTURBO achieves improved reliability and efficiency compared to the classical Turbo decoders in indoor scenarios.
- We provide the interpretation analysis, based on which we conjecture that the weights in TINYTURBO tend to mitigate the over-estimation of beliefs.

## 2 Background

### 2.1 Turbo encoder

Turbo encoder consists of an interleaver and two identical Recursive Systematic Convolutional (RSC) encoders, denoted by  $\pi$  and  $(E_1, E_2)$  respectively, as depicted in Fig. 1. Let  $\mathbf{u} = (u_1, \dots, u_K)$  denote the sequence of  $K$  information bits that we wish to transmit. To encode the message bits  $\mathbf{u}$ , a block of them is directly transmitted via the systematic bit sequence  $\mathbf{x}^s = (x_1^s, x_2^s, \dots, x_K^s)$ . On the other hand, the encoder  $E_1$  generates the parity bit sequence  $\mathbf{x}^{1p} = (x_1^{1p}, x_2^{1p}, \dots, x_k^{1p})$  from  $\mathbf{u}$  whereas the encoder  $E_2$  generates the parity sequence  $\mathbf{x}^{2p} = (x_1^{2p}, x_2^{2p}, \dots, x_k^{2p})$  using the interleaved input  $\tilde{\mathbf{u}} = \pi(\mathbf{u})$ . We assume that the encoded bits  $\mathbf{x} = (\mathbf{x}^s, \mathbf{x}^{1p}, \mathbf{x}^{2p})$  are modulated via Binary Phase Shift Keying (BPSK) and transmitted over the channel. For concreteness, we consider LTE Turbo codes, for which the RSC code has the generator matrix  $(1, g_1(D)/g_2(D))$  with  $g_1(D) = 1 + D^2 + D^3$  and  $g_2(D) = 1 + D + D^3$  [14].

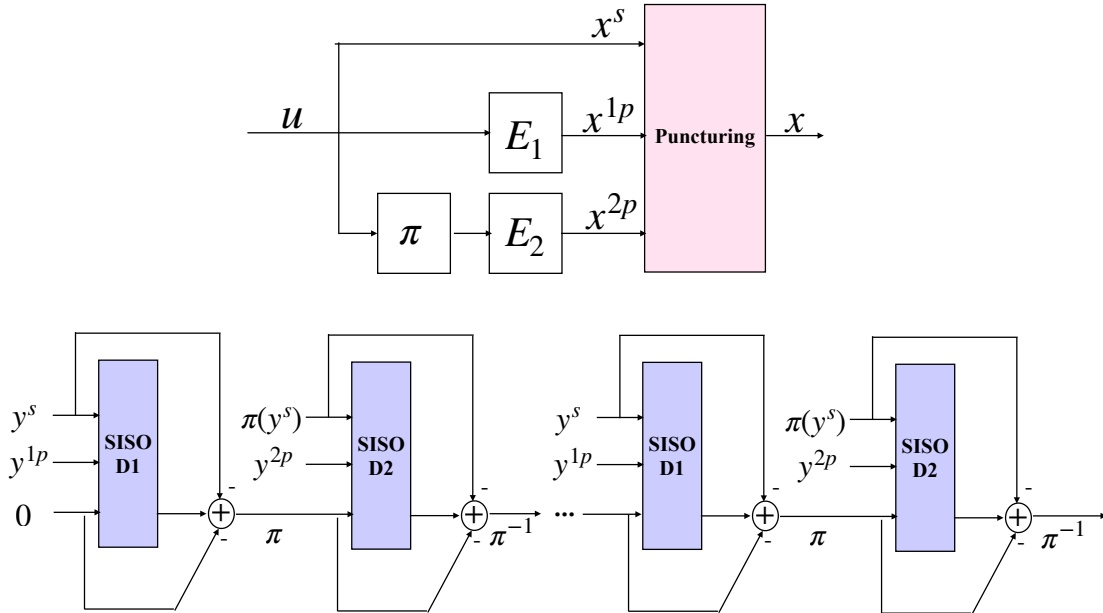


Figure 1: Turbo encoder (top); Turbo decoder (bottom)

### 2.2 Turbo decoder

As depicted in Fig. 1 (bottom), the classical turbo decoder in [1] contains two identical Soft-Input Soft-Output (SISO) decoders ( $D_1, D_2$ ) and relies on the ‘Turbo principle’, where these SISO decoders iteratively refine the posterior of the information bits. More precisely, each SISO decoding block takes the received signals and the prior as input and estimates the posterior distribution for the message bits, which is then fed as a prior for the next SISO decoding block. This procedure is repeated for a fixed number of iterations to estimate the final posterior. For the SISO decoding block, [15] uses the celebrated BCJR algorithm, which we explain below in the context of decoder  $D_1$ .

*MAP turbo decoder:* Let  $\mathbf{y} = (\mathbf{y}^s, \mathbf{y}^{1p})$  be the log-likelihood-ratios (LLRs) of the encoded bits corresponding to encoder  $E_1$ . The BCJR SISO decoder  $D_1$  takes the soft-information  $\mathbf{y}$  as its input and obtains the LLRs for the information bits as follows:

$$L(u_k|\mathbf{y}) \triangleq \log \frac{\mathbb{P}(u_k = 1|\mathbf{y})}{\mathbb{P}(u_k = 0|\mathbf{y})} = \log \frac{\sum_{(s',s) \in S^1} \mathbb{P}(s',s,\mathbf{y})}{\sum_{(s',s) \in S^0} \mathbb{P}(s',s,\mathbf{y})},$$

where  $S^1 = \{(s',s) : u_k = 1\}$  denotes the set of all ordered pairs  $(s',s)$  corresponding to state transitions  $s' \rightarrow s$  caused by data input  $u_k = 1$ , whereas  $S^0 = \{(s',s) : u_k = 0\}$  pertains to the input  $u_k = 0$ . Assuming that the underlying channel is AWGN and memoryless, the joint probabilities  $\mathbb{P}(s',s,\mathbf{y})$  can be efficiently computed:

$$\begin{aligned} \mathbb{P}(s',s,\mathbf{y}) &= \mathbb{P}(s',s,\mathbf{y}_1^{k-1},y_k,\mathbf{y}_{k+1}^K) \\ &= \mathbb{P}(s',\mathbf{y}_1^{k-1}) \mathbb{P}(y_k,s|s') \mathbb{P}(\mathbf{y}_{k+1}^K|s) \\ &= \alpha_{k-1}(s') \gamma_k(s',s) \beta_k(s), \end{aligned}$$

where  $\alpha_{k-1}(s') \triangleq \mathbb{P}(s',\mathbf{y}_1^{k-1})$  and  $\beta_k(s) \triangleq \mathbb{P}(\mathbf{y}_{k+1}^K|s)$  can be computed via the forward and backward recursions [15]:

$$\begin{aligned} \alpha_k(s) &= \sum_{s' \in S_R} \alpha_{k-1}(s') \gamma_k(s',s), \\ \beta_{k-1}(s') &= \sum_{s \in S_R} \beta_k(s) \gamma_k(s',s) \end{aligned}$$

with the initial conditions  $\alpha_0(s) = \beta_K(s) = \mathbb{1}\{s = 0\}$ . Here  $S_R = \{0, 1, \dots, 2^m - 1\}$  denotes the set of all possible states for the encoder whose memory is  $m$ . The branch transition probabilities  $\gamma_k(s',s) \triangleq \mathbb{P}(y_k,s|s')$  can be computed as

$$\gamma_k(s',s) = \exp\left(\frac{1}{2} \left(x_k^s y_k^s + x_k^{1p} y_k^{1p}\right) + \frac{1}{2} u_k L(u_k)\right), \quad (1)$$

where  $L(u_k)$  is the *a priori* LLR for the bit  $u_k$ . Equivalently, by considering the logarithmic values of the above probabilities, i.e.  $\bar{\alpha}_k(s) \triangleq \log \alpha_k(s)$ ,  $\bar{\beta}_k(s) \triangleq \log \beta_k(s)$ , and  $\bar{\gamma}_k(s',s) \triangleq \log \gamma_k(s',s)$ , we obtain

$$\begin{aligned} \bar{\gamma}_k(s',s) &= \frac{1}{2} \left(x_k^s y_k^s + x_k^{1p} y_k^{1p}\right) + \frac{1}{2} u_k L(u_k), \\ \bar{\alpha}_k(s) &= \text{LSE}_{s' \in S_R} (\bar{\alpha}_{k-1}(s') + \bar{\gamma}_k(s',s)), \\ \bar{\beta}_{k-1}(s') &= \text{LSE}_{s \in S_R} (\bar{\beta}_k(s) + \bar{\gamma}_k(s',s)), \\ L(u_k|\mathbf{y}) &= \text{LSE}_{(s',s) \in S^1} (\bar{\alpha}_{k-1}(s') + \bar{\gamma}_k(s',s) + \bar{\beta}_k(s)) \\ &\quad - \text{LSE}_{(s',s) \in S^0} (\bar{\alpha}_{k-1}(s') + \bar{\gamma}_k(s',s) + \bar{\beta}_k(s)) \end{aligned} \quad (2)$$

where  $\text{LSE}(z_1, \dots, z_n) \triangleq \log(\exp(z_1) + \dots + \exp(z_n))$ . Upon obtaining the posterior LLR  $L(u_k|\mathbf{y})$ , the decoder  $D_1$  computes the extrinsic LLR  $L_e(u_k)$  as

$$L_e(u_k) = L(u_k|\mathbf{y}) - L(y_k^s) - L(u_k), \quad k \in [K] \quad (3)$$

which is interleaved and passed as a prior to the decoder  $D_2$ . The posterior  $L^M(u_k|\mathbf{y})$  after the  $M^{\text{th}}$  iteration is used to estimate the message bits:

$$\hat{u}_k = \mathbb{1}\{L^M(u_k|\mathbf{y}) < 0\}$$

### 2.3 Max-log-MAP turbo decoder

The MAP algorithm uses the exact LSE function in the above set of equations in Eq. (2) which is computationally expensive. Hence in practice, several variants and approximations are often used. A popular such decoder is the *max-log-MAP* algorithm. The main idea behind the max-log-MAP is to approximate the LSE function by the maximum:

$$\text{LSE}(z_1, \dots, z_n) \approx \max(z_1, \dots, z_n), \quad z_1, \dots, z_n \in \mathbb{R}.$$

While the max-log-MAP algorithm is more efficient than the MAP, it is less reliable than the MAP [16].

## 2.4 Weighted Max-log-MAP turbo decoder

It is well-known in the literature [17–21] that the max-log-MAP algorithm overestimates the LLRs of the message bits, which leads to propagation of errors in the later decoding stages. To counter this, a common technique is to scale the LLRs in Eq. (3). A variety of methods have been proposed to determine these scaling weights. Most existing works [17–19] propose using heuristics via off-line time-averaged estimates to obtain the best scaling weights for a specific SNR and channel setting. While Claussen et al. [20] propose to find the scaling weights that maximize the mutual information, heuristics are still needed as it is hard to estimate the mutual information. In [21], Sun and Wang use brute force search to find these parameters, which is computationally prohibitive.

## 3 TINYTURBO

In the previous section, we saw the shortcomings of existing turbo decoders. Given this, it would be advantageous to have a set of scaling weights that are both robust across varying block lengths, codes, and channels. *How do we find such weights?*

In a recent work, He et al. [13] introduce TurboNet+, which can be viewed as a weight-augmented version of the max-log-MAP algorithm. TurboNet+ augments the standard max-log-MAP algorithm by adding learnable weights for each bit index  $k \in [K]$  in Eq. (3):  $L_e(u_k) = w_k^{(1)}L(u_k|\mathbf{y}) - w_k^{(2)}y_k^s - w_k^{(3)}L(u_k)$ ,  $k \in [K]$ .

We propose TINYTURBO, a data-driven turbo decoder where the weights in the TurboNet+ architecture are entangled across bit positions. A major difference with TurboNet+ and other existing techniques is that the TINYTURBO efficiently learns the optimal set of weights directly from the data using an *end-to-end loss function*. Learnt in such a purely data-driven manner, we show in Sec. 4 (Fig. 3 and Fig. 4) that these weights yield much better reliability results than the existing baselines and successfully generalize across various channels, block lengths, code rates, and code trellises.

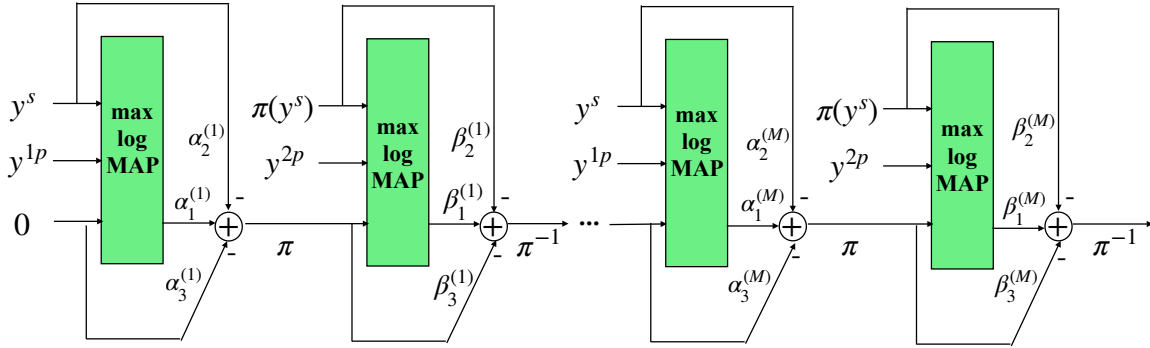


Figure 2: TINYTURBO decoder.

**Architecture.** As depicted in Fig. 2, TINYTURBO generalizes the standard max-log-MAP algorithm by adding just *three* trainable parameters  $\alpha = (\alpha_1, \alpha_2, \alpha_3) \in \mathbb{R}^3$  in the extrinsic LLR computation, i.e.

$$L_e(u_k) = \alpha_1 L(u_k|\mathbf{y}) - \alpha_2 L(y_k^s) - \alpha_3 L(u_k), k \in [K]. \quad (4)$$

Note that the same parameters  $\alpha$  are used for all the bit indices  $k \in [K]$ , making it amenable to generalize across block lengths. Similarly, decoder  $D_2$  has three additional parameters  $\beta = (\beta_1, \beta_2, \beta_3) \in \mathbb{R}^3$ . Thus every decoding iteration in TINYTURBO has 6 parameters  $(\alpha, \beta)$  with the total parameters being  $6M$ , where  $M$  denotes the number of decoding iterations. We consider  $M = 3$  in this paper.

**Training.** We propose an end-to-end loss function framework to train the TINYTURBO parameters  $(\alpha_1^M, \beta_1^M)$ . Hence these weights can be learnt directly from data alone. More precisely, let  $\mathbf{u}^{(1)}, \mathbf{u}^{(2)}, \dots, \mathbf{u}^{(B)} \in \{0, 1\}^K$  denote a batch of  $B$  message blocks each of length  $K$  and let  $\mathbf{y}^{(1)}, \mathbf{y}^{(2)}, \dots, \mathbf{y}^{(B)} \in \mathbb{R}^N$  be the corresponding codeword-LLRs received by the TINYTURBO decoder. Let  $L^M(\mathbf{u}^{(i)}|\mathbf{y}^{(i)}) \in \mathbb{R}^K$  denote the estimated LLRs of the message bits after  $M$  decoding iterations of TINYTURBO for each block  $i \in [B]$ . Define the Binary Cross-Entropy (BCE) loss  $L(\alpha_1^M, \beta_1^M)$

as

$$L(\alpha_1^M, \beta_1^M) \triangleq \frac{1}{B} \sum_{i=1}^B \sum_{k=1}^K u_k^{(i)} \log \sigma(L_k^M(\mathbf{u}^{(i)} | \mathbf{y}^{(i)})) \\ + (1 - u_k^{(i)}) \log \sigma(-L_k^M(\mathbf{u}^{(i)} | \mathbf{y}^{(i)})).$$

The weights  $(\alpha_1^M, \beta_1^M)$  are then trained by running stochastic gradient descent (SGD), or its variants like Adam [22], on the loss  $L$ . The hyper-parameters for training are shown in Table 1 below. Once trained, these weights are frozen and are used directly for inference (turbo decoding).

Loss	BCE
Optimizer	Adam with initial LR = 0.0008
Batch size	1000
Training SNR	-1 dB
Number of iterations	5000

Table 1: Training hyperparameters

**Comparison with TurboNet+.** While TINYTURBO is similar to TurboNet+, the following are the key differences: (a) TurboNet+ introduces weights for each bit index  $k \in [K]$  in Eq. (3). As shown in Table 2, they have a total of  $6MK$  parameters, as opposed to just  $6M$  for TINYTURBO; (b) For training the weights, they consider a mean square error (MSE) between their estimated LLRs and the target BCJR-LLRs, which are obtained by running the MAP algorithm for BCJR. This introduces a computational overhead and makes the training slow as BCJR-LLRs are required for each training iteration; (c) Since the weights are learned for each bit index  $k \in [K]$ , they cannot be reused for longer block lengths. In contrast, we show that by using just a  $1/K$ -fraction of weights and an end-to-end loss function, TINYTURBO learns a better set of weights that yield better reliability performance on various practical channels (Fig. 4). Further, our decoder generalizes better across a variety of scenarios (Fig. 3).

Block length	40	200
TINYTURBO	<b>18</b>	<b>18</b>
TurboNet+	720	3600

Table 2: Number of parameters of TINYTURBO is independent of block length

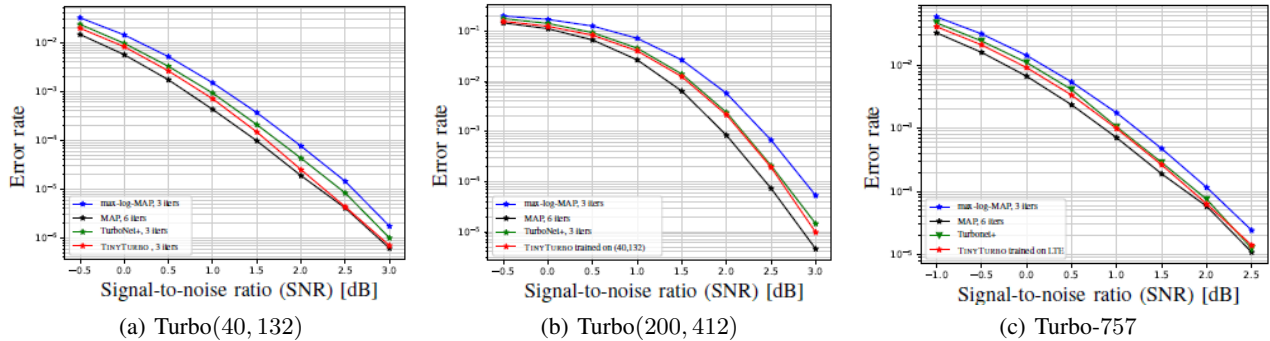


Figure 3: AWGN results: (a) TINYTURBO trained on Turbo (40, 132) outperforms the baselines and is close to MAP; (b) & (c) TINYTURBO generalizes to different block lengths, code rates, and trellises.

## 4 Results

We compare the performance of TINYTURBO with that of the standard max-log-MAP and MAP turbo decoders, and TurboNet+ [23]. We consider rate-1/3 and rate-1/2 Turbo-LTE codes of block length 40 and 200, and use the standard Quadratic Permutation Polynomial (QPP) interleaver [14].

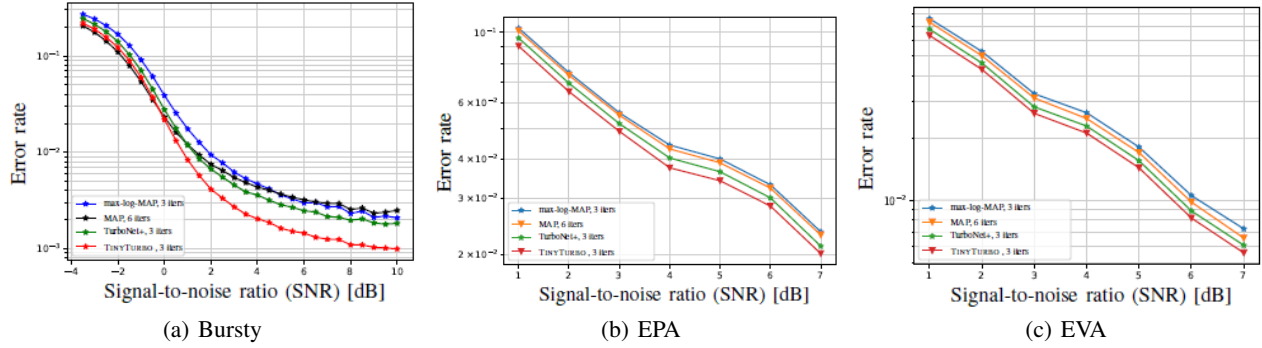


Figure 4: Robustness: TINYTURBO exhibits strong robustness than baselines on practical channels: Bursty, EPA and EVA

#### 4.1 AWGN channel

We train the TINYTURBO for Turbo(40, 132) on the AWGN channel at  $-1$  dB. Using these weights, we evaluate the performance of TINYTURBO on the following three codes under AWGN: Turbo(40, 132), Turbo-757, and Turbo(200, 412). As highlighted in Figs. 3(a), 3(b), and 3(c), TINYTURBO with 3 decoder iterations achieves a bit error rate (BER) performance close to that of the MAP decoder with 6 iterations. Further, we achieve this with a decoding complexity comparable to a max-log-MAP decoder. We also note that TINYTURBO outperforms TurboNet+ even with  $40\times$  fewer parameters.

#### 4.2 Generalization to other blocklengths, rates, and trellises.

One of the major shortcomings of learning-based decoders is that training them directly on larger block lengths is generally difficult due to insufficient GPU memory, and unstable training [24–27]. It is thus ideal to have models that are trained on short block lengths and are reusable for longer ones. Indeed, as illustrated in Fig. 3(b), we observe that TINYTURBO trained on a small code, Turbo(40, 132), shows good performance when tested on a Turbo code of block length 200. Interestingly, we also notice that a TINYTURBO model trained directly on block length 200 achieves similar performance. These results highlight that our model seamlessly generalizes to longer block lengths.

Puncturing is a technique used to encode and decode codes of higher rates using standard rate  $1/3$  encoders and decoders. Higher rates are achieved by removing certain parity bits according to a fixed pattern. The use of puncturing improves the flexibility of a system without significantly increasing its complexity. As shown in Figure 3(b), the weights learned using a rate  $1/3$  Turbo code can be reused for a rate  $1/2$  punctured Turbo code, which demonstrates the generalizability of TINYTURBO across code rates. Surprisingly, TINYTURBO also generalizes well to different trellises; Fig. 3(c) shows that TINYTURBO trained on Turbo-LTE achieves a BER performance close to MAP even on a Turbo-757 code with the generator matrix  $(1, 1 + D^2 / 1 + D + D^2)$ .

#### 4.3 Robustness across channel variations

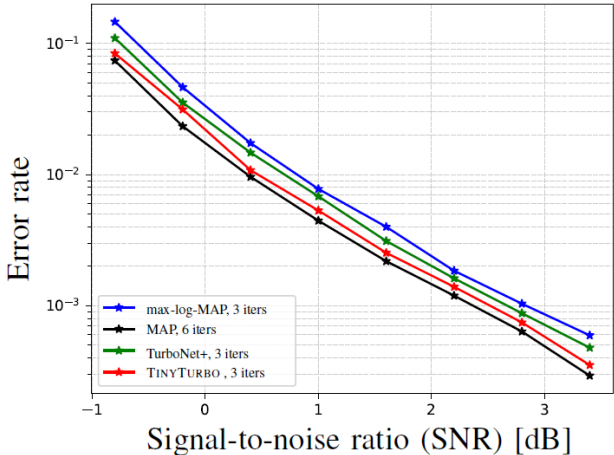
Here we evaluate the TINYTURBO decoder trained on AWGN on various non-AWGN settings (without any retraining). We consider both the simulated and practical channels.

We first test on a bursty channel, defined as  $y = x + z + w$ , where  $z \sim \mathcal{N}(0, \sigma_1^2)$  is an AWGN noise, and  $w \sim \mathcal{N}(0, \sigma_b^2)$  is a bursty noise with a high noise power and low probability of occurrence  $\rho$ . Here we consider  $\sigma_b = 5$  and  $\rho = 0.01$ . Fig. 4(a) highlights that TINYTURBO is significantly more robust to the bursty noise compared to the canonical Turbo decoders.

We now demonstrate the robustness of TINYTURBO on various practical channels. In particular, we consider the multi-path fading channels, as defined in the 3GPP [28]. We simulate them using the LTE toolbox in MATLAB. Specifically, we test on the Extended Pedestrian A model (EPA) and the Extended Vehicular A model (EVA) specified in the LTE standard. The EPA and EVA channels represent a low and medium delay spread environment respectively. The received signals are equalized using linear MMSE estimation before proceeding to decode. As shown in Figures 4(b) and 4(c), TINYTURBO achieves better reliability than the MAP Turbo decoder on the EPA and EVA channels.

## 5 Over-the-air

In this section, we use a rapid prototype system with a ZynQ SoC and an AD9361 transceiver as a testbed to evaluate the performance of our TINYTURBO algorithm in a practical setting. We implement these algorithms on the ZynQ CPU and the FPGA with an OFDM-based end-to-end communication system. Specifically, we analyze the robustness of our algorithm due to the multipath channel variations and showcase the practical viability of the algorithms on transceiver chips. In a real-time processing system, we use two of these systems as transmitter and receiver, to transmit and capture frames. The Turbo-encoded codewords were modulated and sent over the channel after adding a preamble for synchronization and frequency offset correction. The received data was equalized and demodulated to get LLR values for the decoder. Simulations were done over different gain settings at the transmitter and the receiver to get the results for different SNRs. As demonstrated in Figure 5, TINYTURBO is robust to multipath fading.



## 6 Interpretation and Ablation Study

### 6.1 Interpreting TINYTURBO

In Sections 4 and 5, we have demonstrated that TINYTURBO\* can achieve much better reliability than the baseline turbo decoders across a variety of channels. This raises a natural question: *where do these gains come from?* To this end, we fix the input message bits to be the all-zero vector and examine the corresponding LLR values predicted by TINYTURBO and our baselines for Turbo(40,132). In Fig. 5 (left), we consider the AWGN channel and plot the mean LLR together with the error bars corresponding to two standard deviations. While all the decoding algorithms have a negative mean LLR since the message bits are all-zero, only TINYTURBO and MAP decoders can keep the deviations close to/lesser than zero resulting in fewer errors. On the other hand, max-log-MAP has a significant portion of zero crossings and hence more decoding errors. These observations are consistent with our AWGN results in Fig. 3(a).

We consider a simplified bursty channel model  $y = x + z + w$ , where  $x, y, z$  are as described in Section 4.3, and  $w = 10.0$  only at the  $57^{th}$  symbol in the 132-length zero codeword. Figure 5 (right) illustrates that only TINYTURBO can keep the deviations contained below zero, whereas the baselines have lots of zero crossings resulting in poor decoding performance. This explains the superior performance of TINYTURBO as demonstrated in Fig. 4(a).

	$\alpha_1$	$\alpha_2$	$\alpha_3$	$\beta_1$	$\beta_2$	$\beta_3$
Iteration 1	0.445	0.584	1	0.641	0.779	0.662
Iteration 2	0.834	0.795	0.725	0.863	0.716	0.645
Iteration 3	0.911	0.715	0.638	0.263	0.616	0.938

Table 3: TINYTURBO weights

### 6.2 Ablation study

The key differences between TINYTURBO and TurboNet+ are: (i) weights are shared across bit positions for TINYTURBO unlike TurboNet+, and (ii) TINYTURBO minimizes the BCE loss between the predicted LLRs and the ground

\*The learned weights are shown in Table 3.

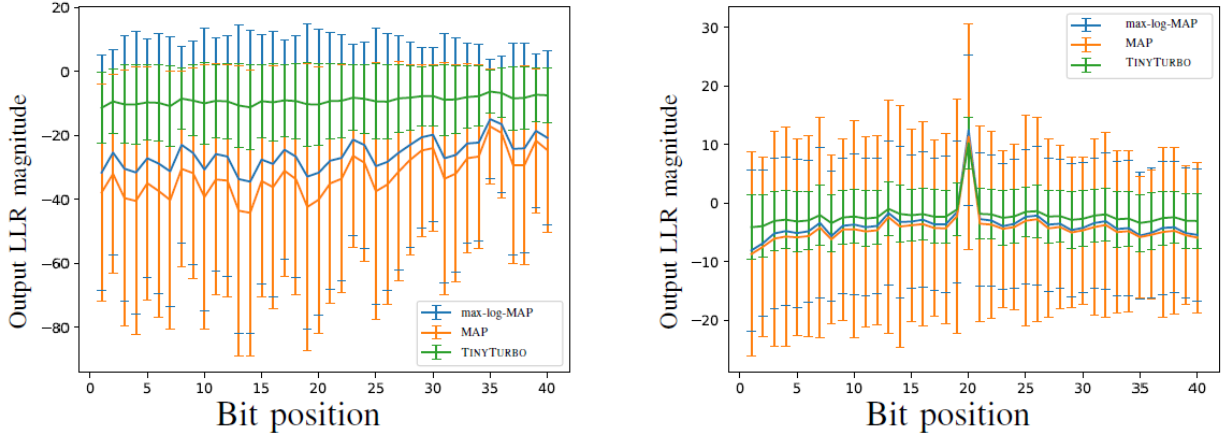


Figure 5: Average output LLRs on AWGN (left) and bursty (right) channels

truth message bits; TurboNet+ minimizes the MSE loss between the estimated LLRs and the BCJR-LLRs from the MAP algorithm. We evaluate the contributions of these components to our gains using the following ablation experiments: (i) we do not entangle weights across bit positions in TINYTURBO but train them using BCE loss. The resulting red curve in Figure 6 highlights that this approach has the same performance as that of TINYTURBO. (ii) we entangle weights but train them using the same procedure as TurboNet+. The corresponding purple curve in Figure 6 shows similar performance as TurboNet+. Together, these experiments suggest that training the weights via the end-to-end BCE loss function approach is the key contributing factor to the gains of TINYTURBO over TurboNet+. While sharing weights did not yield any change in the performance, it nonetheless allows for a more computationally efficient decoder with a low-memory requirement.

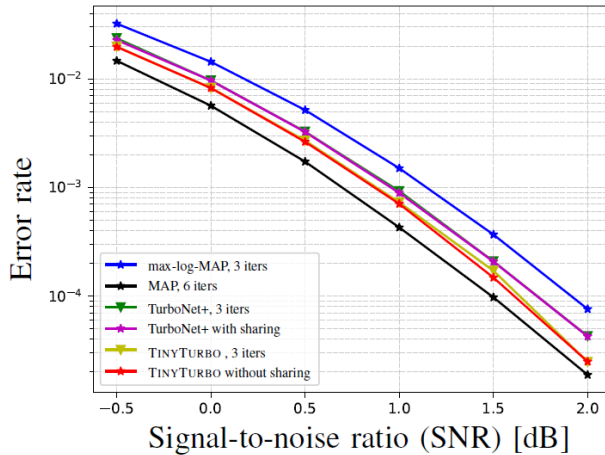


Figure 6: Turbo(40, 132). Our gains are mainly due to the end-to-end BCE loss function.

## 7 Acknowledgement

This work was supported by ONR grants W911NF-18-1-0332, N00014-21-1-2379, NSF grant CNS-2002932, Intel, and the affiliates of the 6G@UT center within WNCG at UT Austin.



---

## References

- [1] C. Berrou, A. Glavieux, and P. Thitimajshima, “Near shannon limit error-correcting coding and decoding: Turbo-codes. 1,” in *Proceedings of ICC’93-IEEE International Conference on Communications*, vol. 2. IEEE, 1993, pp. 1064–1070.
- [2] E. Nachmani, Y. Be’ery, and D. Burshtein, “Learning to decode linear codes using deep learning,” in *2016 54th Annual Allerton Conference on Communication, Control, and Computing (Allerton)*, 2016, pp. 341–346.
- [3] T. Gruber, S. Cammerer, J. Hoydis, and S. ten Brink, “On deep learning-based channel decoding,” in *2017 51st Annual Conference on Information Sciences and Systems (CISS)*. IEEE, 2017, pp. 1–6.
- [4] H. Kim, Y. Jiang, R. Rana, S. Kannan, S. Oh, and P. Viswanath, “Communication algorithms via deep learning,” *arXiv preprint arXiv:1805.09317*, 2018.
- [5] H. Kim, S. Oh, and P. Viswanath, “Physical layer communication via deep learning,” *IEEE Journal on Selected Areas in Information Theory*, 2020.
- [6] B. Vasić, X. Xiao, and S. Lin, “Learning to decode ldpc codes with finite-alphabet message passing,” in *2018 Information Theory and Applications Workshop (ITA)*. IEEE, 2018, pp. 1–9.
- [7] F. Liang, C. Shen, and F. Wu, “An iterative bp-cnn architecture for channel decoding,” *IEEE Journal of Selected Topics in Signal Processing*, vol. 12, no. 1, pp. 144–159, 2018.
- [8] C.-F. Teng, C.-H. D. Wu, A. K.-S. Ho, and A.-Y. A. Wu, “Low-complexity recurrent neural network-based polar decoder with weight quantization mechanism,” in *ICASSP 2019-2019 IEEE International Conference on Acoustics, Speech and Signal Processing (ICASSP)*. IEEE, 2019, pp. 1413–1417.
- [9] A. Buchberger, C. Häger, H. D. Pfister, L. Schmalen, and A. G. Amat, “Pruning neural belief propagation decoders,” in *2020 IEEE International Symposium on Information Theory (ISIT)*. IEEE, 2020, pp. 338–342.
- [10] X. Chen and M. Ye, “Cyclically equivariant neural decoders for cyclic codes,” *arXiv preprint arXiv:2105.05540*, 2021.
- [11] N. Shlezinger, J. Whang, Y. C. Eldar, and A. G. Dimakis, “Model-based deep learning,” *arXiv preprint arXiv:2012.08405*, 2020.
- [12] Z. Qin, H. Ye, G. Y. Li, and B.-H. F. Juang, “Deep learning in physical layer communications,” *IEEE Wireless Communications*, vol. 26, no. 2, pp. 93–99, 2019.
- [13] Y. He, J. Zhang, S. Jin, C.-K. Wen, and G. Y. Li, “Model-driven dnn decoder for turbo codes: Design, simulation, and experimental results,” *IEEE Transactions on Communications*, vol. 68, no. 10, pp. 6127–6140, 2020.
- [14] 3GPP, “LTE; Evolved Universal Terrestrial Radio Access (E-UTRA); Multiplexing and channel coding,” 3rd Generation Partnership Project (3GPP), Technical Specification (TS) 36.212, 01 2011, version 10.0.0. [Online]. Available: <https://www.3gpp.org/>
- [15] L. Bahl, J. Cocke, F. Jelinek, and J. Raviv, “Optimal decoding of linear codes for minimizing symbol error rate (corresp.),” *IEEE Transactions on information theory*, vol. 20, no. 2, pp. 284–287, 1974.
- [16] W. Ryan and S. Lin, *Channel codes: classical and modern*. Cambridge university press, 2009.
- [17] J. Vogt and A. Finger, “Improving the max-log-map turbo decoder,” *Electron. Lett.*, vol. 36, pp. 1937–1939, 2000.
- [18] J. N. C. Chaikalis and F. Riera-Palou, “Improving the reconfigurable sova/log-map turbo decoder for 3gpp,” *IEEE / IEE International Symposium on Communication Systems, Networks and DSP*, 2002.
- [19] N. H. Yue DW, “Unified scaling factor approach for turbo decoding algorithms,” *IET Commun.*, pp. 905–914, 2010.
- [20] H. Claussen, H. Karimi, and B. Mulgrew, “Improved max-log map turbo decoding using maximum mutual information combining,” in *14th IEEE Proceedings on Personal, Indoor and Mobile Radio Communications, 2003. PIMRC 2003.*, vol. 1, 2003, pp. 424–428 Vol.1.
- [21] L. Sun and H. Wang, “Improved max-log-map turbo decoding by extrinsic information scaling and combining,” in *Communications, Signal Processing, and Systems*, Q. Liang, X. Liu, Z. Na, W. Wang, J. Mu, and B. Zhang, Eds. Springer Singapore, 2020, pp. 336–344.
- [22] D. P. Kingma and J. Ba, “Adam: A method for stochastic optimization,” 2017.
- [23] Y. He, J. Zhang, S. Jin, C.-K. Wen, and G. Y. Li, “Model-driven dnn decoder for turbo codes: Design, simulation, and experimental results,” *IEEE Transactions on Communications*, vol. 68, no. 10, pp. 6127–6140, 2020.

- 
- [24] Y. Jiang, S. Kannan, H. Kim, S. Oh, H. Asnani, and P. Viswanath, “Deepturbo: Deep turbo decoder,” in *2019 IEEE 20th International Workshop on Signal Processing Advances in Wireless Communications (SPAWC)*. IEEE, 2019, pp. 1–5.
- [25] M. Ebada, S. Cammerer, A. Elkelesh, and S. ten Brink, “Deep learning-based polar code design,” in *2019 57th Annual Allerton Conference on Communication, Control, and Computing (Allerton)*. IEEE, 2019, pp. 177–183.
- [26] Y. Jiang, H. Kim, H. Asnani, S. Kannan, S. Oh, and P. Viswanath, “Learn codes: Inventing low-latency codes via recurrent neural networks,” *IEEE Journal on Selected Areas in Information Theory*, 2020.
- [27] A. V. Makkuva, X. Liu, M. V. Jamali, H. MahdaviFar, S. Oh, and P. Viswanath, “Ko codes: inventing nonlinear encoding and decoding for reliable wireless communication via deep-learning,” in *International Conference on Machine Learning*. PMLR, 2021, pp. 7368–7378.
- [28] 3GPP, “Evolved Universal Terrestrial Radio Access (E-UTRA); User Equipment (UE) Radio Transmission and Reception.” 3rd Generation Partnership Project (3GPP), Technical Specification (TS) 36.104, 04 2017, version 14.3.0. [Online]. Available: <https://www.3gpp.org/>